Brillouin Scattering from a Homogeneous 1,4-Polyisoprene–Poly(vinylethylene) Diblock Copolymer and Its Constituent Homopolymers

J. Kanetakis, G. Fytas,* and N. Hadjichristidis†

Foundation for Research and Technology—Hellas, Institute of Electronic Structure and Laser, P.O. Box 1527, 711 10 Heraklion, Crete, Greece

Received June 7, 1990; Revised Manuscript Received September 4, 1990

ABSTRACT: Polarized Rayleigh–Brillouin Spectroscopy (BS) has been used to probe the local segmental dynamics at hypersonic frequencies in a homogeneous 1,4-polyisoprene–1,2-polybutadiene diblock copolymer far from the microphase separation transition (MST) and the corresponding homopolymers. An Arrhenius temperature dependence along with an exponential decay of the structural relaxation times τ_s provides an adequate fit of the experimental longitudinal loss modulus M'', which reveals a similar dynamics in the diblock and 1,4-polyisoprene but at variance with the dynamics in 1,2-polybutadiene (poly(vinylethylene)). On the contrary, recent photon correlation spectroscopy (PCS) data obtained in the same materials near and above T_g indicate a much broader distribution of relaxation times in the diblock than in the constituent homopolymers. Moreover, a Vogel–Fulcher–Hesse–Tammann equation cannot describe reasonably both the low-temperature (PCS) and high-temperature (BS) data. The combined results of the PCS and BS measurements in the present homogeneous diblock copolymer with a single T_g indicate that a difference in segmental mobilities and shape parameters β (with regard to the conventional Kohlrausch–Williams–Watts equation) may explain the behavior of the diblock near and above T_g, while at high temperatures where BS applies, a fast single relaxation time process seems to be responsible for the similar hypersonic dispersion in the diblock and homopolymer. These measurements represent a first, to our knowledge, application of dynamic light scattering methods to probe the dynamic behavior of homogeneous diblocks.

Introduction

Block copolymer melts exhibit interesting compatibilizing[1] and surface-active properties,[2] undergo unique phase transitions, and produce a variety of morphologies[3] that have attracted the attention of polymer scientists for many years. Static structural properties have been the subject of significant research work, employing various experimental techniques among which small-angle scattering of neutrons (SANS)[4,5] and X-rays (SAXS)[6] are more frequently used. Most of these properties are mainly determined by local interactions between segments of the chemically dissimilar chains and the degrees of polymerization of the blocks, N_A and N_B. An important success of the mean field theory, known also as the random phase approximation (RPA), is the prediction of the phase diagram, from which the Flory–Huggins effective interaction parameter χ can be determined.[7] While symmetric ($N_A = N_B = N/2$) binary polymer mixtures are homogeneous when $\chi N < 4$, symmetric diblock copolymers are in the homogeneous region of the phase diagram as long as the looser condition $\chi N < 10.5$ is fulfilled. The composition fluctuations, specific to blends and copolymers, have amplitude and correlation length that depend[8] on χN. The spatial inhomogeneity is of the order of the macromolecular size ($\sim R_g$) for microphase-separated diblock copolymers and assumes macroscopic scales in phase-separated polymer mixtures.[9]

In the disordered phase, the amplitude of the concentration fluctuations decreases with decreasing χN and is predicted to be very small with microscopic length scale in the context of RPA. Hence, local segmental dynamics should reflect random mixing of the two blocks in the homogeneous phase. Alternatively, correlation in concentration fluctuations can lead to local inhomogeneities that may exert an excess effect on segmental dynamics. Spectroscopic techniques, sensitive to local dynamic structure, are able to provide useful information concerning segment–segment interactions on this scale. Few investigations have appeared in the literature on segmental dynamics in homogeneous diblock copolymers.[10,11] In four 1,4-polybutadiene (PBD)–poly(vinylethylene) (PVE) diblocks, dielectric spectroscopy (DR)[10] has recently revealed two distinct primary (α) glass–rubber relaxations even in samples that are homogeneous ($\chi N \sim 5$) on the scale of SANS, calorimetric, and rheological measurements. Large-amplitude composition fluctuations in regions rich in each component were inferred from these resolved relaxations in contrast to the usual mean field assumption.[7] Homogeneous PBD–PVE diblocks[12] exhibit a single albeit broad glass transition, the width of which has also been related with phase segregation effects, i.e., proximity to microphase transition. In contrast, the breadth of the glass transition in compatible 1,4-polyisoprene (PIP)/PVE blends[13] was unrelated to phase morphology. Local interactions should, in principle, be the same in both homogeneous binary polymer mixtures and block copolymers. It has been observed[14] that while blends of two homopolymers are clearly heterogeneous, diblocks of the corresponding homopolymers may be homogeneous materials, with the magnitude of χN being the crucial factor in determining miscibility.

Recently, photon correlation spectroscopy[15] (PCS) over the time range 10^{-6}–10^{2} s was employed to study the primary relaxation in a PIP–PVE ($N = 107$) diblock copolymer in the disordered state near the glass transition temperature, T_g. The spectrum of relaxation times extracted from the density correlation function $g(t)$ was unusually broader in PIP–PVE than in the corresponding pure homopolymers. The blocks in PIP–PVE ($\chi \sim 0.2 \times 10^{-3}$)[13,16] are considerably more miscible than those in PBD–PVE ($\chi \sim 6 \times 10^{-3}$),[12,17] and the former copolymer ($N = 107$) should be far from the microphase separation transition (MST). The width of the distribution observed

† Also at the Department of Industrial Chemistry, University of Athens, 10680 Athens, Greece.

0024-9297/91/2224-1806$02.50/0

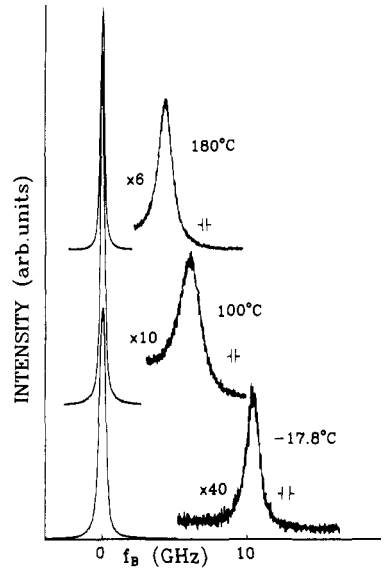

Figure 1. Polarized Rayleigh Brillouin spectra of the PIP–PVE diblock at three different temperatures. The spectra at T = 180 and 100 °C were obtained with FSR = 21.44 GHz and the spectrum at -17.8 °C with FSR = 33.4 GHz. The instrumental full width is indicated by vertical bars.

in PIP–PVE may therefore reflect differences between the segmental mobilities of the two blocks.

In this paper, we extend the time-domain PCS measurements to higher T using the frequency-domain Brillouin scattering method (BS) at gigahertz frequencies over the T range -40 to +180 °C. As the relevant correlation function probed by both light scattering experiments is $g(t)$, it is interesting to examine the hypersonic dispersion which is also associated with local segmental dynamics. This first, to our knowledge, application of BS to diblock copolymer melts shows that subtle composition fluctuations in a homogeneous PIP–PVE diblock far from MST have a minor effect on the Brillouin doublet at high T. The analysis of the Brillouin spectra reveals a very similar segmental dynamics in PIP and the diblock copolymer but at variance with the dynamics in PVE.

Experimental Section

A. Brillouin Scattering. The Rayleigh–Brillouin spectra were obtained in the VV scattering configuration at a scattering angle of 90° using a piezoelectrically scanned single-pass plane Fabry–Perot interferometer. The Burleigh DAS-10 stabilization system was used to maintain finesse and stabilize cavity separation. The spectra were taken with free spectral ranges 21.44, 22.45, 27.82, and 33.4 GHz, and the typical operating finesse was about 65. After repetitive averaging, two spectral orders were stored in a multichannel analyzer (Canberra Series 35 plus) and transferred to a VAX mainframe computer. The excitation source was an argon ion laser operating at single mode selected with an intracavity etalon from the 488-nm emission line. The incident power at the sample was about 150 mW.

Rayleigh–Brillouin spectra were obtained at temperatures ranging between -43.6 and +160 °C for 1,4-polyisoprene (PIP), between -42.2 and +200 °C for 1,2-polybutadiene (PVE), and from -31.7 to +180 °C for the PIP–PVE diblock copolymer. The Brillouin doublets in the region uninfluenced by the Rayleigh line were fitted with a nonlinear estimation routine based on Marquardt's compromise and employing a Lorentzian function to describe each of the Brillouin lines as well as a background. The full width at half-height Γ_B was obtained after correcting for the instrumental line width. Typical spectra of the diblock at three temperatures are shown in Figure 1.

B. Materials. A poly(1,4-isoprene-*b*-1,2-butadiene) diblock copolymer of weight-average molecular weight M_w 6400 was purchased from Polymer Standards Service, Mainz, Germany.

Table I
Sample Characteristics

sample	structure	$w_{1,4}$[a]	M_w	M_w/M_n	T_g,[c] °C
PIP	1,4 homopolymer	1[b]	2350	1.10	-66.6
PVE	1,2 homopolymer	0	90000		5.6
PIP–PVE	1,4–1,2 diblock	0.49	6407	1.03	-52.3

[a] Weight fraction of polyisoprene block. [b] Microstructure: 93% 1,4 (66% cis-1,4, 27% trans-1,4), 7% 3,4. [c] 20 °C/min heating rate.

The mass fraction for isoprene is 0.49, determined through weighing of educts. The GPC characterization was done in dried THF stored under argon, and a polyisoprene calibration was used. The copolymer contains 0.01% antioxidant and was used without further purification.

The 1,4-polyisopropene samples (66% cis-1,4, 27% trans-1,4, and 7% 3,4) with M_w = 2350 and the 1,2-polybutadiene sample with M_w = 90 000 were synthesized at Exxon Chemical Co., NJ. The samples contain approximately 0.5% antioxidant. Molecular characteristics of all the samples, where available, are listed in Table I. To remove the antioxidant from the homopolymers, samples were dissolved in *n*-hexane, precipitated from methanol, cooled with liquid nitrogen, in which way the pure homopolymers were easily removed, and then dried under vacuum. The resulting samples were of good optical quality for laser light scattering. Dust-free samples were obtained by filtration of the polymer solution in *n*-hexane through a 0.22-μm Millipore filter into a dust-free scattering cell, followed by slow evaporation of the solvent in a vacuum oven for several weeks. During this procedure, temperature was not allowed to exceed 50 °C. The cells were then flame sealed under vacuum. The glass transition temperatures were determined by differential scanning calorimetry (Perkin-Elmer DSC 7, Mettler DSC30). The T_g values for the three samples at a heating rate of 20 °C/min are listed in Table I.

C. Auxiliary Measurements. Refractive indices n were measured with an Abbé refractometer (Type 3T) in the temperature range 10–60 °C. The dependence of n on temperature is given by the following relations: $n = 1.522 - 3.91 \times 10^{-4}T$ (°C) for PIP, $n = 1.508 - 3.64 \times 10^{-4}T$ (°C) for PVE, and $n = 1.514 - 3.86 \times 10^{-4}T$ (°C) for the diblock. For PIP the temperature dependence of density ρ was estimated by using $\rho(25\,°C) = 0.899$ g/cm^3 [18] and the volume expansion coefficient $\alpha = (1/V)(\partial V/\partial T) = 6.7 \times 10^{-4}$ K^{-1}.[19] For PVE, $\rho(25\,°C) = 0.89$/cm^3, as reported for polybutadienes with a high level of 1,2 microstructure.[20] At other temperatures, densities of PVE were calculated by using the reported value of the thermal expansion coefficient $\alpha = -\mathrm{d}\ln\rho/\mathrm{d}T = 0.75 \times 10^{-3}$ °C^{-1}.[21] Density for the diblock was calculated as an average value of the densities of the two homopolymers.

Results

Polarized Brillouin scattering of the multicomponent fluid arises mainly from local thermal density fluctuations; concentration fluctuations have a minor direct effect on the hypersonic dispersion.[22] The Brillouin spectrum at a scattering angle θ, is determined by the qth mode of the Fourier transform of the density autocorrelation function $g(\mathbf{q},t)$. $\mathbf{q}$ is the scattering wave vector with magnitude $q = (4\pi/\lambda)n \sin\theta/2$, with λ the wavelength of the incident light in vacuo and n the refractive index of the medium. In the phenomenological approach to the Brillouin scattering one measures the dispersion of the longitudinal modulus[23] M^* ($=M' + iM''$). The storage modulus M' is associated with the hypersonic velocity u ($=\omega_B/q$) whereas the loss modulus M'' is related to the Brillouin full width Γ_B according to ($\omega_B \gg \Gamma_B$)

$$M' = \rho u^2 \tag{1a}$$

$$M'' = (\Gamma_B/\omega_B)M' \tag{1b}$$

where ρ is the density. Table II summarizes the hyper-

Table II
Hypersonic Velocity[a] and Brillouin Full Width[b] for the Three Polymer Samples

	1,4-polyisoprene (PIP)		PIP–PVE diblock		1,2-polybutadiene (PVE)	
T, °C	υ, m/s	Γ_B, GHz	υ, m/s	Γ_B, GHz	υ, m/s	Γ_B, GHz
200					951	0.91
180			1038	0.76	1006	1.08
160	1094	0.65	1103	0.93	1098	1.23
140	1153	0.81	1181	1.08	1195	1.31
130			1227	1.19		
120	1229	1.03	1292	1.26	1308	1.34
110			1336	1.31		
100	1316	1.31	1413	1.36	1439	1.22
90			1470	1.41		
80	1459	1.52	1547	1.39	1580	1.10
70			1622	1.35		
60	1613	1.53	1704	1.30	1724	1.01
40	1762	1.35	1867	1.09	1887	0.90
30	1845	1.14				
22	1905	1.06		0.81		
20			2010		2046	0.73
-1	2106	0.72	2201	0.57	2245	0.69
-17.4					2308	0.56
-17.8			2345	0.48		
-18.3	2247	0.53				
-31.7			2449	0.35		
-42.2					2351	0.47
-43.6	2453	0.32				

[a] Experimental error was not greater than ±2% for sound velocity. [b] Experimental error was not greater than ±7% for line width.

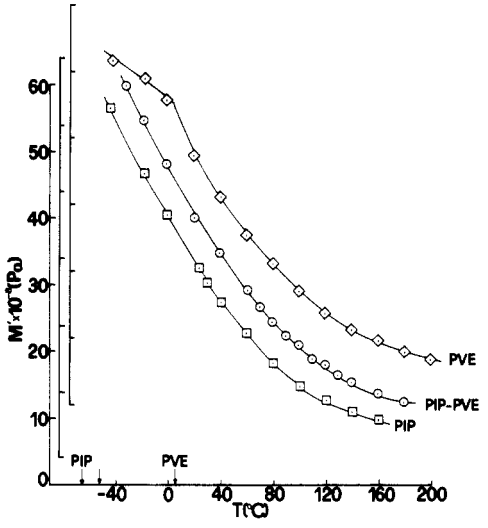

Figure 2. Longitudinal storage modulus M' versus temperature for the three polymers. The arrows denote the conventional glass transition temperatures. The origin of the M' axis for PIP–PVE and PVE has been shifted upward to avoid coincidence of the M' values. Note the characteristic kink displayed by the PVE curve at T_g.

sonic velocity and line widths for the three samples. The material properties M' and M'' for the present PIP, PIP–PVE, and PVE are plotted versus T in Figures 2 and 3, respectively. Brillouin shifts and widths have previously been reported[24] for bulk PIP (T_g = −73 °C) and PVE (T_g = −13 °C) over the T range 20–150 °C. These data (ω_B, M''/M') display very similar features to those of the present homopolymers, which moreover exhibit much lower Landau–Placzek intensity ratio.

A few pertinent differences may be gleaned from glancing at the data of Figures 2 and 3. PVE displays the characteristic kink in the Brillouin shift at $T \approx T_g$. The temperature T^*, at which M'' has its maximum value, assumes quite similar values in the three samples despite

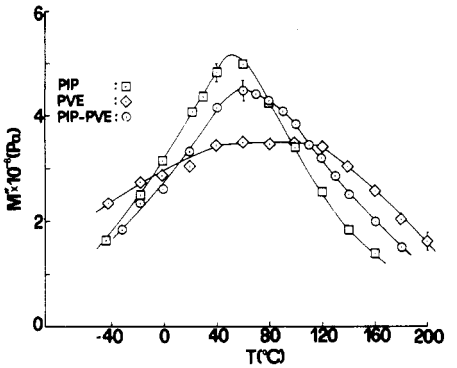

Figure 3. Longitudinal loss modulus M'' versus temperature for the three polymers under study.

the much larger difference in their T_g's. The M'' peak is much broader in PVE whereas it displays a similar shape in the PIP and PIP–PVE copolymer. We discuss these interesting differences and similarities in the following section.

Discussion

Distribution of Relaxation Times. It has been recently shown that the dynamic longitudinal compliance D'' is related to the normalized density correlation function $g(t) \equiv \langle \delta\rho_q(t)\delta\rho_q^*(0)\rangle / \langle|\delta\rho_q(0)|^2\rangle$ by[25]

$$D''(\omega) = \omega(D_0 - D_\infty)\int_0^\infty \cos(\omega t)\, g(t)\, dt \qquad (2)$$

where D_0 and D_∞ are the low- and high-frequency limiting D' values. The compliance D'' is connected with the experimentally observable moduli M' and M'' (eq 1) via the well-known equation[26]

$$D'' = \frac{M''}{(M')^2 + (M'')^2} \qquad (3)$$

The two different approaches employed to analyze hypersonic data from Brillouin measurements at $T > T_g$ are nowadays in debate: a stretched exponential $g(t)$ non-Arrhenius temperature dependence of the structural relaxation times $\tau(T)$[28-30] versus an exponential $g(t)$.[27] In the conventional Brillouin experiment, one usually measures $M'(T)$ and $M''(T)$ as a function of T at a frequency ω_B which varies also with T. The knowledge of $\tau(T)$ and/or the relaxation function $g(t)$ is therefore very crucial for an unambiguous representation of the hypersonic data by eqs 2 and 3 with a minimum number of adjustable parameters. According to the first approach, BS and photon correlation spectroscopy (PCS) probe the same segmental process, and consequently the $\tau(T)$ can be deduced from the longitudinal relaxation times τ_M at low T near T_g (PCS) and high T (BS) according to the well-known Vogel–Fulcher–Hesse–Tammann (VFHT) free-volume equation:[26]

$$\tau = \tau_0 \exp(B/(T - T_0)) \qquad (4)$$

The experimental values of τ used in the fitting procedure were consistently defined as $\tau_M = 1/\omega^*$ at T^* at which M'' has its maximum value. For the frequency-domain BS experiment, τ_M is obtained from the location of the $M''(T)$ maximum (Figure 3). On the other hand, for the time-domain PCS experiment which measures directly the relaxation function $g(t)$, the following transformations were carried through. First, via eq 2 we obtained the frequency ω^* at which $D''(\omega)$ attains its maximum values. For non-exponential $g(t)$, ω^* is greater than $1/\langle\tau\rangle$, with $\langle\tau\rangle$ being the average relaxation time of $g(t)$; for single relaxation

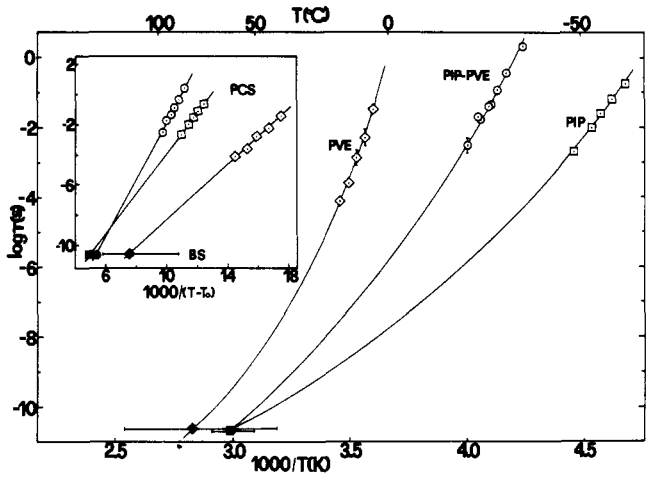

Figure 4. Logarithm of relaxation time τ plotted versus inverse of temperature for the PCS (open symbols) and BS (solid symbols) data. The non-Arrhenius temperature dependence is illustrated in the insert. Solid lines represent fits to the VFHT equation (eq 4).

time τ, $\omega^* = 1/\tau$. Second, since the real part M' is greater than M'' by at least an order of magnitude (Figures 2 and 3) and it does not change significantly with frequency compared with $M''(\omega)$, $D''(\omega)$ and $M''(\omega)$ obtain their maximum values at virtually the same ω^* according to eq 3.

Figure 4 shows the T dependence of τ_M for the three polymers. The non-Arrhenius behavior can be described by eq 4 as illustrated in the insert of the same figure. The solid lines are based on the equations $\tau = 4.4 \times 10^{-18} \exp[3082/(T - 133.6)]$ for PIP, $\tau = 1.4 \times 10^{-21} \exp[4360/(T - 147.1)]$ for PIP–PVE, and $\tau = 2.5 \times 10^{-18} \exp[2130/(T - 220.5)]$ for PVE, where T is in K. With regard to the physical meaning of the VFHT parameters, we should notice the relatively small intercept τ_0 and the disparity in the value of B for the three polymes. By means of the derived temperature dependences of the relaxation times τ for the three samples, one can compute the reduced loss $D''/(D_0 - D_\infty)$ from eq 2, provided the functional form of $g(t)$ is known.

The measured $g(t)$ for the bulk homopolymers near T_g conforms to the well-known Kohlrausch–Williams–Watts (KWW) decay function $g(t) = \exp[-(t/\tau)^\beta]$ with distribution parameter $\beta = 0.40 \pm 0.02$ and $\beta = 0.35 \pm 0.02$ for PIP and PVE, respectively. In Figure 5 we compare the normalized experimental M''/M''_{max} values with the computed values of D''/D''_{max} obtained with this procedure for PIP and PIP–PVE. The dashed lines correspond to $\beta = 0.4$, and it is obvious that agreement between experimental and computed values has not been achieved even for this low β value. For PVE, in order to describe the broader $M''(T)$ peak (Figure 3) an even lower β is required. However, for the few known cases so far, β invariably increases[31] with increasing T toward $\beta = 1$, which corresponds to a single relaxation time decay. Apparently, a nonexponential $g(t)$ with a strong non-Arrhenius dependence of eq 4 cannot describe the measured $M''(T)$. The hypersonic dispersion in poly(propylene glycol) (PPG)[28] and its complexes with various salts[29,30] has been invariably described by eq 3 using $\beta \approx 0.4$ and assuming the three parameters in eq 4. This is however a strong assumption that exerts a large influence on the β value and hence renders the peak analysis ambiguous. It is noteworthy that the estimation of β from the maximum attenuation[29] is subject to large errors; possible contributions from relaxation processes other than the primary structural relaxation have been neglected.

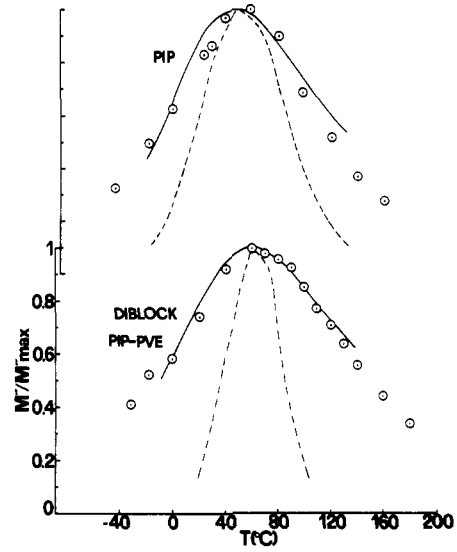

Figure 5. Normalized loss modulus M''/M''_{max} versus temperature for the diblock and PIP. Open circles denote experimental values. Dashed lines correspond to computed values according to eq 3 with $\beta = 0.4$. Solid lines correspond to solution of eq 6 employing relaxation times τ_s near the maximum. For more details, see text.

Single Relaxation Time. We turn now to the second approach, which assumes that an exponential $g(t)$ describes the hypersonic dispersion $M^*(T)$ via a weaker temperature dependence of τ_s extracted from

$$M' - M_0 = M_r\omega^2\tau_s^2/(1 + \omega^2\tau_s^2) \quad (5)$$

$$M'' = M_r\omega\tau_s/(1 + \omega^2\tau_s^2) \quad (6)$$

where M_r ($=M_\infty - M_0$) is the difference between the high- and low-frequency limiting M' values. Since M_0 can be estimated with better precision than M_r (or equivalently M_∞), we have chosen to compute τ_s from $\tau_s = (M' - M_0)/\omega M''$ using only experimental quantities near T^*. The limiting M_0 ($=u_0^2\rho$) has been calculated from the velocity data at high T. We have thus obtained $u_0 = 1529 - 2.73T$ (°C) for PIP and the diblock and $u_0 = 1497 - 2.73T$ (°C) for PVE. The $\tau(T)$ obtained in this way is well described by an Arrhenius equation which in turn is used to compute the theoretical M''/M''_{max} from eq 6. This procedure was found to be an adequate description of the hypersonic attenuation in bulk PIP and the diblock PIP–PVE. For the former $\tau_s = 2.2 \times 10^{-13} \exp(1657/T)$, whereas for the copolymer $\tau_s = 3.8 \times 10^{-13} \exp(1589/T)$. Figure 5 illustrates the comparison between computed (eq 6) and experimental normalized loss modulus for PIP and PIP–PVE. Notwithstanding the uncertainty of the absolute $M''(T)$ values, owing to possible contributions from other relaxational processes, the present data rather favor a crossover from a clearly nonexponential at low T to a quasi-exponential $g(t)$ at high T (and hence high ω). This behavior is in accord with theoretical calculations[32,33] and experimental findings.[31] We support this conjecture more in the last section.

For PVE, the dispersion region of $M''(T)$ is stretched out over an unusually wide T range, indicating either a slowly changing $\tau(T)$ or the presence of more than one mechanism that causes hypersonic attenuation. Its breadth can still be accounted for by an exponential $g(t)$; however, the resulting $\tau(T)$ exhibits a very weak T dependence ($E_a \sim 1.6$ kcal/mol). On the other hand, a lower activation energy B (eq 4) in PVE than in PIP was reported for the mechanical shift factor in the softening region as a result of the lower segmental friction[26] in PVE than in PIP when

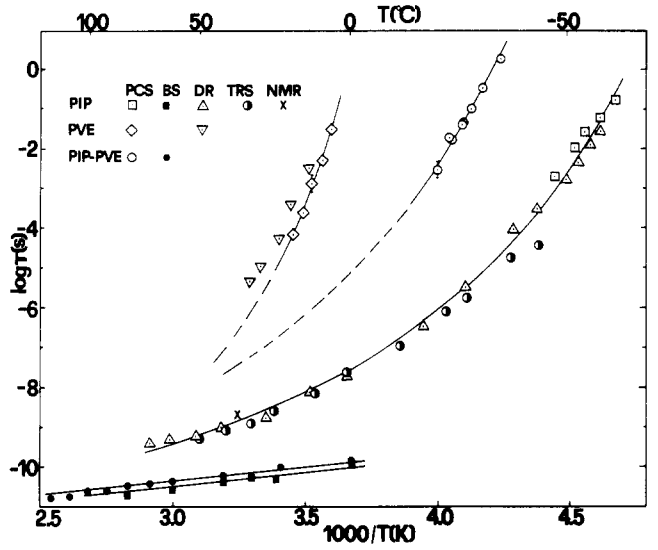

Figure 6. Logarithm of relaxation times τ from various experimental techniques plotted as a function of inverse temperature for the three polymers under investigation. The lines through the Brillouin scattering (BS) data (solid symbols) represent fits of the structural relaxation times $\tau_s = (M' - M_0)/\omega M''$ (eqs 5 and 6) to an Arrhenius equation. The solid line through PIP, which includes results other than BS, represents fit of the PCS[15] and dielectric relaxation[40] data to the VFHT equation (eq 4). The dashed–solid lines through PVE and PIP–PVE represent fits of the PCS[15] data to eq 4. For more details, see text.

compared at T equidistant from their T_g's. The difference in the segmental frictions between PIP and PVE might be of the same origin as that observed between PVE and PBD; in the latter it has been speculated[26] that the origin is the double bond in the chain backbone of the 1,4 configuration (PBD). In addition, recent dielectric relaxation (DR) measurements[10] have shown the presence of a less T-dependent secondary relaxation process in PVE assigned to the vinyl side group. In this context, it is interesting to mention that in the series of poly(alkyl methacrylates) the width of $\Gamma_B(T)$ was found to increase by increasing the length of the side group.[34] Despite these complications that preclude a quantitative description of the hypersonic dispersion in PVE, the present Brillouin data clearly show that PVE loses its separate identity in the PIP–PVE copolymer; the width ΔT of $M''(T)$ peak is definitely not a molar average of the ΔT's of the pure components. This finding at high T is evidently at variance with the far broader shape of $g(t)$ for PIP–PVE near T_g than for the parent homopolymers.[15]

This broader distribution of relaxation times in the diblock can originate either from correlations in local composition fluctuations leading to heterogeneities[10,35] or from a difference between the segmental mobilities[13] of the two components. Whereas the former mechanism is not strongly T dependent ($\sim T^{-1}$), the latter difference diminishes at high T because the segmental mobilities usually exhibit a VFHT T dependence. If the first mechanism were operational, then the $M''(T)$ for the copolymer at high T would have displayed a broader shape than the parent homopolymers. Conversely, the second mechanism is in accord with the experimental shapes of $g(t)$ and $M''(T)$ at low and high T, respectively, provided that the same primary relaxation is probed. However, the Brillouin data of Figure 5 show that a quasi-exponential $g(t)$ provides a more suitable representation of the hypersonic dispersion, and hence the resulting $\tau_s(T)$ is at variance with eq 4. Figure 6 visualizes the comparison between $\tau_s(T)$ at high T and primary relaxation times from PCS measurements near T_g. It is evident from Figure 6 that the hypersonic data for the three samples are faster than the predicted values from the VFHT equation. Similar behavior is displayed by other systems: polybutadiene[36] when PCS, ultrasonic, and BS data are interrelated, PPG,[37] and other molecular glass formers.[38]

The Arrhenius and VFHT dependences (to be discussed in the last section) in Figure 6 suggest the presence of two different relaxation processes with time scales that tend to merge at very high T. In the context of the coupling model of relaxation,[33] the crossover from a KWW to a single relaxation time decay function seems to occur at the low edge of gigahertz frequencies. In this framework, the observed similarities between PIP and PIP–PVE in Figures 3–5 indicate that the secondary relaxation in PVE is eliminated (either plasticized or depressed) in PIP–PVE block copolymer. It has been previously reported that blending of polycarbonate can impact the secondary relaxation.[39] Parenthetically, at low T the time scales of the primary and secondary relaxations are well separated, and only the former process dominates $g(t)$, which thus reveals differences in segmental mobility.[15] The glass transitions of PIP/PVE compatible mixtures ($\chi_F \sim 2 \times 10^{-4}$) were found to exhibit a significant broadening when the more glassy component (PVE) was present in high concentration.[13] The breadth of the glass transition was thus unrelated to phase segregation effects. The broad shape of $g(t)$ near T_g reflects similar mobility effects and probably differences between the values of the distribution parameter β in the homopolymers.

Alternatively, an enhancement for the secondary (β) relaxation of PVE was observed in the microphase-separated diblock PBD–PVE[10] ($\chi_F \sim 6 \times 10^{-3}$). If this enhancement were due to the plasticization introduced by PBD, then an even stronger β relaxation would have been observed in the homogeneous PBD–PVE diblocks in which the composition of PBD within the PVE-rich regions is higher. To account conclusively for these findings further studies of PIP–PVE diblocks with different compositions and chain lengths are needed. Nevertheless, the present study demonstrates the first application of Brillouin spectroscopy to study structural rearrangements in a PIP–PVE homogeneous diblock copolymer.

Comparison with Other Techniques. In Figure 6 we compare the relaxation times determined from dynamic light scattering techniques with the results of other techniques probing primary and secondary relaxations. For PIP the solid curve represents a fit of our PCS data at low temperatures with the dielectric relaxation data by Boese et al.[40] according to the VFHT equation (eq 4), where $\log \tau_0 = -12.6 \pm 0.6$ (τ_0 in seconds), $B = 1177.3 \pm 208.0$ K, $T_0 = 171.4 \pm 6.3$ K, and correspondingly $c_2^g = 35.2 \pm 6.3$ K. For their dielectric study Boese et al. report values of $B = 1050$ K and $T_0 = 170$ K, and from mechanical measurements Gotro et al.[18] report $c_2^g = 30.4$ K.

It is obvious that at low T the PCS data follow closely the DR results when all the times are defined as $1/\omega^*$, where ω^* is the frequency at which the mechanical and dielectric loss have their maximum value. Here it is noteworthy that the distribution parameter β of the KWW decay function for both polarized PCS and DR experiments is experimentally the same ($\beta = 0.4$). Also plotted along the solid VFHT curve are data from time-resolved optical (TRS) experiments of Hyde et al.,[41] by which the rotational dynamics of small molecules embedded in bulk polyisoprene are probed. At high temperatures and down to approximately −14 °C the TRS results follow the DR data,

but at lower temperatures TRS underestimates the time obtained by PCS and DR. In a subsequent study, Hyde et al.[42] report results of the same method applied to study the local segmental dynamics of anthracene-labeled PIP. However, the results of these two studies are quite different, the time being much longer with the labeled chains. In addition, the times obtained with the labeled PIP chains[42] are longer than the DR times.[40] Shown also in the curve is the correlation time from NMR measurements of Howarth.[43] For a predominantly cis PIP, secondary relaxations should be very weak as shown by dynamic mechanical measurements[44] and by PCS measurements.[15]

The line through the 1,2-polybutadiene (PVE) data represents the fit to a VFHT equation of the PCS data using c_2^g = 39.8 K (T_0 = 239 K) as reported by Carella et al.,[20] which then results in log $\tau_0 = -13.2 \pm 0.8$ (in seconds) and $B = 1054.7 \pm 85$ K. The dielectric α-relaxation data reported by Quan et al.[10] for 1,2-polybutadiene (PVE) of M_N = 48 000 follow quite closely the PCS line. This DR study has shown that PVE exhibits a quite broad and weak secondary transition attributed to the local motion of the vinyl side group. However, it is very difficult to assign a peak to this broad transition, and it is even more formidable to find its temperature dependence. In fact, in view of the present Brillouin data these secondary times appear to merge with the primary relaxation at relatively low T and hence at long times. Therefore, we decided not to include these data in Figure 6. Unlike the situation in PIP, the shape of the density time correlation functions for PVE[15] indicates the presence of fast secondary process.

For the copolymer PIP-PVE there do not exist other results besides the present BS data to compare with the PCS data. We have used a fixed c_2^g = 35.7 K (T_0 = 185.2 K) equal to the value in PIP and found log $\tau_0 = -13.0 \pm 1.0$ (in seconds) and $B = 1582.6 \pm 131$ K for the parameters of the VFHT equation. Notwithstanding the relatively narrow T range, the extrapolation at high T near T^* of the maximum hypersonic attenuation predicts faster relaxation times in PIP than in the diblock at lesat by a factor of 10. In contrast, the Brillouin experiments reflect very similar dynamics in these polymers, with PIP being only slightly faster. Again, this comparison strengthens further the conjecture that fast single relaxation time processes, exhibiting an Arrhenius T dependence, cause hypersonic dispersion at high T.

For PIP at high T, DR arises from segmental orientation[40] due to the dipole moment perpendicular to the chain contour, and the autocorrelation function of the perpendicular dipole moment component displays a nonexponential decay characterized by β = 0.40. In this context, it is interesting to mention that frequency-domain depolarized Rayleigh spectra of PIP are clearly non single Lorentzian lines. The orientational relaxation time τ_{or} determined from the maximum dielectric loss is longer than τ_s ($=1/\omega^*_B$) at T^* by a factor of 10. Hence, orientational relaxation is not effective in causing hypersonic attenuation in PIP because the condition $\omega_B\tau_{or} \gg 1$ holds (see eq 6). The present situation resembles that of poly(propylene glycol) in which both DR and Brillouin data are compared at the same T. The T variation of the Brillouin spectra at gigahertz frequencies therefore reflects the relaxation of the bulk modulus K rather than the shear modulus G ($M^* = K^* + {}^4/_3G^*$). In the model of "hierarchically constrained dynamics"[45] the short relaxation time τ_s probably characterizes the fast degrees of freedom with an exponential response. In the framework of the coupling model of relaxation,[33] τ_s can be identified with the relaxation of the primitive species τ_0, and the relaxation function is again exponential.

The disparity between τ_{or} and τ_s at high T is not in contradiction with the same nonexponential shape of the density and orientational time correlation functions and their similar relaxation times at low T near T_g as revealed by the analysis of the Rayleigh peak by PCS.[46] These findings have suggested a strong coupling between translational and rotational motions near T_g. It is also known that at low T bulk and shear modulus have similar magnitude, and hence the volume and shear relaxation times are quite close.

Conclusions

A homogeneous 1,4-polyisoprene-1,2-polybutadiene (PIP-PVE) diblock copolymer far from the microphase separation transition and the corresponding homopolymers PIP and PVE have been investigated by the Rayleigh-Brillouin scattering (BS) method, and their behavior at hypersonic frequencies has been compared with recent photon correlation spectroscopy (PCS) measurements performed on the same samples. These complementary dynamic light scattering methods, probing the same density autocorrelation function $g(t)$, are able to give insight into the local dynamics of the diblock from very low temperatures (PCS) close to T_g up to high temperatures where BS applies. While near and above T_g the shape of $g(t)$ as probed by PCS clearly differentiates the behavior of the diblock as compared to the two homopolymers, at high temperatures the experimentally observable longitudinal modulus M^* shows no effective broadening in the case of the diblock. This comparison shows that fast single relaxation time processes exhibiting an Arrhenius temperature dependence cause hypersonic dispersion at high T.

We have not been able to observe any effect of local concentration inhomogeneities in the copolymer. Difference in the segmental mobilities and in the value of the distribution parameter β of the two blocks may explain the unusually very broad distribution of relaxation times of the diblock close to T_g. However, at high temperatures where the segmental dynamics are probed by BS, the friction coefficients of the two blocks, which normally follow the VFHT temperature dependence, approach each other, and the segmental dynamics reflect no more mobility differences. In order to further elucidate the dynamic behavior of homogeneous diblocks, studies of copolymers with different block fractions are needed.

Acknowledgment. The financial support of the Volkswagen Stiftung (No. I/62872) and the Foundation for Research and Technology—Hellas is gratefully appreciated.

References and Notes

(1) Anastasiadis, S. H.; Gancarz, I.; Koberstein, J. T. *Macromolecules* **1989**, *22*, 1449.
(2) Anastasiadis, S. H.; Russel, T. P.; Satija, S. J.; Majkrzak, C. F. *Phys. Rev. Lett.* **1989**, *62*, 1852.
(3) Folkes, M. J., Ed. *Processing, Structure and Properties of Block Copolymers*; Elsevier: New York, 1985.
(4) Bates, F. S.; Hartney, M. A. *Macromolecules* **1985**, *18*, 2478.
(5) Fischer, E. W.; Jung, W. G. *Makromol. Chem., Macromol. Symp.* **1989**, *26*, 179.
(6) Owens, J. N.; Gancarz, I. S.; Koberstein, J. T.; Russell, T. P. *Macromolecules* **1989**, *22*, 3380.
(7) Leibler, L. *Macromolecules* **1980**, *13*, 1602.
(8) Fredrickson, G. H.; Helfand, E. *J. Chem. Phys.* **1987**, *87*, 697.
(9) de Gennes, P.-G. *Scaling Concepts in Polymer Physics*; Cornell University Press: Ithaca, NY, 1979.

(10) Quan, X.; Johnson, G. E.; Anderson, E. W.; Bates, F. S. *Macromolecules* **1989**, *22*, 2451.
(11) Stühn, B.; Rennie, A. R. *Macromolecules* **1989**, *22*, 2460.
(12) Bates, F. S.; Bair, H. E.; Hartney, M. A. *Macromolecules* **1984**, *17*, 1987.
(13) Trask, C. A.; Roland, C. M. *Macromolecules* **1989**, *22*, 256.
(14) Cohen, R. E.; Ramos, A. R. *Macromolecules* **1979**, *12*, 131.
(15) Kanetakis, J.; Fytas, G.; Pakula, T.; Kremer, F., to be published.
(16) Roland, C. M. *Macromolecules* **1987**, *20*, 2557.
(17) Cohen, R. E.; Wilfong, D. E. *Macromolecules* **1982**, *15*, 370.
(18) Gotro, J. T.; Graessley, W. W. *Macromolecules* **1984**, *17*, 2767.
(19) Brandrup, J.; Immergut, E. H., Eds. *Polymer Handbook*, 2nd ed.; Wiley: New York, 1975.
(20) Carella, J. M.; Graessley, W. W.; Fetters, L. J. *Macromolecules* **1984**, *17*, 2775.
(21) Saunders, J. F.; Valentine, R. H.; Ferry, J. D. *J. Polym. Sci., Part A-2* **1965**, *6*, 967.
(22) Berne, B. J.; Pecora, R. *Dynamic Light Scattering*; Wiley: New York, 1976; Chapter 10.
(23) Pinnow, D. A.; Candau, S. J.; LaMacchia, J. T.; Litovitz, T. A. *J. Acoust. Soc. Am.* **1968**, *43*, 131.
(24) Jarry, J.-P.; Patterson, G. D. *J. Polym. Sci., Polym. Phys. Ed.* **1981**, *19*, 1791.
(25) Wang, C. H.; Fischer, E. W. *J. Chem. Phys.* **1985**, *82*, 632. Meier, G.; Hagenah, J.-U.; Wang, C. H.; Fytas, G.; Fischer, E. W. *Polymer* **1987**, *28*, 1640.
(26) Ferry, J. D. *Viscoelastic Properties of Polymers*; Wiley: New York, 1980.
(27) Lin, Y.-H.; Wang, C. H. *J. Chem. Phys.* **1978**, *69*, 1546; **1979**, *70*, 681. Torell, L. M. *J. Chem. Phys.* **1987**, *28*, 1803. Ngai, K. L.; Rendell, R. W.; Wang, C. H. *Polymer* **1989**, *30*, 369.
(28) Börjesson, L.; Stevens, J. R.; Torell, L. M. *Polymer* **1987**, *28*, 1803.
(29) Sandahl, J.; Schantz, S.; Börjesson, L.; Torell, L. M.; Stevens, J. R. *J. Chem. Phys.* **1989**, *91*, 655.
(30) Sandahl, J.; Börjesson, L.; Stevens, J. R.; Torell, L. M. *Macromolecules* **1990**, *23*, 163.
(31) Fytas, G.; Wang, C. H.; Lilge, D.; Dorfmüller, Th. *J. Chem. Phys.* **1981**, *75*, 4247. Dixon, P. K.; Nagel, S. R. *Phys. Rev. Lett.* **1988**, *61*, 341. Cheng, L.-T.; Yan, Y.-X.; Nelson, K. A. *J. Chem. Phys.* **1989**, *91*, 6052.
(32) Fredrickson, G. H.; Brawer, S. A. *J. Chem. Phys.* **1986**, *84*, 3351. Campbell, I. A.; Flesselles, J.-M.; Jullien, R.; Botet, R. *Phys. Rev.* **1988**, *B37*, 3825.
(33) Ngai, K. L.; Wang, C. H.; Fytas, G.; Plazek, D. L.; *J. Chem. Phys.* **1987**, *86*, 4768.
(34) Li, B. Y.; Jiang, D. Z.; Fytas, G.; Wang, C. H. *Macromolecules* **1986**, *19*, 778.
(35) Wetton, R. E.; MacKnight, W. J.; Fried, J. R.; Karasz, F. E. *Macromolecules* **1978**, *11*, 158.
(36) Floudas, G.; Fytas, G.; Alig, I. *Polymer*, in press.
(37) Yano, S.; Rahalkar, R. R.; Hunter, S. P.; Wang, C. H.; Boyd, R. H. *J. Polym. Sci., Polym. Phys. Ed.* **1976**, *14*, 1877.
(38) Wang, C. H.; Fytas, G.; Zhang, J. *J. Chem. Phys.* **1985**, *82*, 3405.
(39) Pochan, J. M.; Gibson, H. W.; Froix, M. F.; Hinman, D. F. *Macromolecules* **1978**, *11*, 165.
(40) Boese, D.; Kremer, F. *Macromolecules* **1990**, *23*, 829.
(41) Hyde, P. D.; Ediger, M. D. *Macromolecules* **1989**, *22*, 1510.
(42) Hyde, P. D.; Ediger, M. D.; Kitano, T.; Ito, K. *Macromolecules* **1989**, *22*, 2253.
(43) Howarth, O. W. *J. Chem. Soc., Faraday Trans. 2* **1980**, *76*, 1219.
(44) Morgan, R. J.; Nielsen, L. E.; Buchdahl, R. *J. Appl. Phys.* **1971**, *42*, 4653.
(45) Palmer, R. G.; Stein, D. L.; Abrahams, E.; Anderson, P. W. *Phys. Rev. Lett.* **1984**, *53*, 958.
(46) Wang, C. H.; Fytas, G.; Lilge, D.; Dorfmüller, Th. *Macromolecules* **1981**, *14*, 1363.

Registry No. (PIP)(PVE) (block copolymer), 109264-12-2; PIP (homopolymer), 9003-31-0; polybutadiene (homopolymer), 9003-17-2.